INFLUENCE OF EXPERIMENTAL BOUNDARY CONDITIONS ON KINETIC MODELS FOR FIRE SPREAD PREDICTION

Felix Armbrust[1], Tristan Hehnen[2], Jochen Zehfuß[1], Olaf Riese[1] und Lukas Arnold[2,3]

[1] Institute of Building Materials, Concrete Construction and Fire Safety (iBMB), Center of Fire Research (ZeBra), Technische Universität Braunschweig, Braunschweig
[2] Chair of Computational Civil Engineering, University of Wuppertal, Wuppertal
[3] Institute for Advanced Simulation, Forschungszentrum Jülich, Jülich

INTRODUCTION

Fire growth and flame spread models are widely used in performance-based fire safety engineering. In current practice, these models are typically used to evaluate the consequences of design fire scenarios defined by prescribed sources of mass, energy, and momentum. While effective for scenario-based assessments, their predictive capability is limited to the predefined conditions. A main objective in fire science is to develop physically based models where the fire dynamics emerge from the intrinsic properties of the combustible material and the prevailing boundary conditions. However, this remains challenging due to insufficient coupling between condensed-phase pyrolysis and gas-phase combustion and uncertainties in parameter determination [1].

Pyrolysis models are pivotal in fire modelling as they govern decomposition and gas release, which drive fire growth and flame spread. To represent these processes, both chemical kinetics and heat and mass transfer within the condensed phase could be relevant. The required input data are classified into kinetic, thermodynamic, and transport properties [1, 2]. A complete description should specify whether reactions are consecutive or parallel and the yields of intermediate and final products.

Kinetic parameters are usually determined through micro-scale experiments such as thermogravimetric analysis (TGA), differential scanning calorimetry (DSC), and micro-scale combustion calorimetry (MCC) [2-7]. These methods involve exposing a specimen to a heating programme while measuring a property versus time, e.g. mass loss or heat release rate, and also measuring the temperature. Such experiments assume that heat and mass transfer effects are negligible, corresponding to a zero-dimensional (0D) model.

There is still no consensus on how pyrolysis parameters should be derived for reliable predictions of fire growth and flame spread. Numerous studies [2,3,8-12] and initiatives such as the Measurement and Computation of Fire Phenomena (MaCFP) working group [13] have addressed this, yet major uncertainties persist, largely due to the absence of standardised experimental protocols. The wide variation in methods reduces reproducibility and comparability, while boundary

conditions such as sample mass, sample geometry, heating rate and purge gas flow strongly affect the measured response [5,14]. When heat and mass transfer are not negligible, systematic errors are introduced into the derived parameters. These issues are reinforced by the flexibility of current thermoanalytical and calorimetric standards, which allow diverse configurations and conditions [7,15,16]. This enables testing of a broad range of materials but undermines consistency across studies. Among experimental parameters, specimen preparation is particularly critical: ideally, geometry should reflect the intended application (e.g. slab tests for sheet materials), while powders are often chosen for reduced gradients and improved repeatability [17]. The impact of preparation is further illustrated by DiDomizio and McKinnon, who demonstrated that cryo-milling duration alters the decomposition of PMMA powder, showing that even minor variations can shift kinetic parameters [18]. No conclusion was reached on how to best prepare the samples. A valid methodology for parameter determination still needs to be established in the fire-science community. In contrast, the International Confederation for Thermal Analysis and Calorimetry (ICTAC) was able to reach a consensus, which was published in its recommendations [14].

This study demonstrates how experimental boundary conditions influence the outcomes of micro-scale experiments and how the fundamental assumptions required for deriving kinetic parameters can be ensured. Polymethyl methacrylate (PMMA) was used as the sample material. Thermogravimetric analysis (TGA) under varying conditions provided the mass-loss data, complemented by evolved gas analysis (EGA) for mechanistic insights. Since factors such as sample configuration influence decomposition behaviour, separate kinetic models were developed for piece and powder configurations. These models were then subjected to a consequence analysis using the Fire Dynamics Simulator (FDS) to highlight the implications of experimental and modelling choices.

THEORY

The derivation of kinetic parameters from thermoanalytical data relies on the classical framework of thermal analysis. The experimental programme in this study was designed according to ICTAC recommendations. The theoretical basis of kinetic modelling and the influence of experimental boundary conditions are briefly summarised in the following.

Kinetic Modelling of Thermal Decomposition

Kinetic modelling describes dynamic processes in which physical quantities evolve over time. The degree of conversion is expressed by α, which in the case of thermal decomposition usually refers to the mass [14]:

$$\alpha(t) = \frac{\Phi_0 - \Phi(t)}{\Phi_0 - \Phi_\infty} \tag{1}$$

Φ_0 is the initial, $\Phi(t)$ the instantaneous and Φ_∞ the final value of the property. The process rate $\mathrm{d}\alpha/\mathrm{d}t$ depends mainly on temperature, process progression and pressure [19]:

$$\frac{\mathrm{d}\alpha}{\mathrm{d}t} = k(T) f(\alpha)\, h(p) \tag{2}$$

The rate constant $k(T)$ reflects the temperature dependency and is often expressed by an Arrhenius approach that incorporates the pre-exponential factor (A), the activation energy (E), the universal gas constant (R) and the material temperature T. The function $f(\alpha)$ represents the reaction model. Common types include sigmoidal (autocatalytic), decelerating and accelerating behaviours [19]. In most studies, the pressure dependency $h(p)$ is neglected. A single-step process can then be described by [14]:

$$\frac{\mathrm{d}\alpha}{\mathrm{d}t} = A \exp\left(\frac{-E}{RT}\right) f(\alpha) \tag{3}$$

A, E *and* $f(\alpha)$ build the kinetic triplet and define the full kinetic system [20]. For the determination of the kinetic triplet, multiple strategies exist. While model-free methods are typically employed for single-step processes, model-fitting approaches are generally more suitable for multi-step processes [19,21-24].

The integral form of the general rate equation is obtained by integration of the differential rate law (Eq. 3) and substitution of the time variable using the relationship $\beta = \mathrm{d}T/\mathrm{d}t$, which applies under non-isothermal and constant heating rate conditions [19]:

$$g(\alpha) = \frac{A}{\beta} \int_0^T \exp\left(\frac{-E}{RT}\right) \tag{4}$$

$g(\alpha)$ denotes the integral form of the reaction model, β the constant heating rate.

This equation is the basis for isoconversional (or model-free) methods. At fixed α, the rate depends only on temperature, so the conversion dependent activation energy (E_α) can be determined without prior mechanistic assumptions [25].

Isoconversional analysis can be used to distinguish single- from multi-step processes. In single-step reactions, E_α is nearly constant across $0.05 \leq \alpha \leq 0.95$ [19]. Deviations below 10–20 % are generally interpreted as single-step behaviour [25]. For polymers, overlapping mechanisms such as chain scission, depolymerisation or side-group elimination are common; isoconversional methods provide a quantitative criterion of such complexity [26,27].

Here, the Kissinger-Akhaira-Sunose (KAS) method is applied – a more accurate isoconversional approach than the Osawa-Flinn-Wall method – which relies on an approximation of the temperature integral [19,28].

$$\ln\left(\frac{\beta_i}{T_{\alpha,i}^{B}}\right) = \text{const} - C\left(\frac{E_\alpha}{RT_\alpha}\right) \tag{5}$$

The slope of $\ln(\beta/T^B)$ versus $1/T$ gives E_α. The constants depend on the chosen approximation (e.g. Starink: B = 1.92, C = 1.0008) [28].

For multi-step kinetics, each step requires its own kinetic triplet and possible interactions must be considered [29,30]:

$$\frac{\mathrm{d}\alpha}{\mathrm{d}t} = \sum_i c_i \frac{\mathrm{d}\alpha_i}{\mathrm{d}t} \tag{6}$$

c_i represents the individual contribution of step i to the overall process. If the steps are independent, the total rate equation simplifies to [20]:

$$\frac{\mathrm{d}\alpha}{\mathrm{d}t} = \sum_i c_i\, A_i \exp\left(\frac{-E_i}{RT}\right) f_i(\alpha_i) \tag{7}$$

The number of steps can be inferred from peaks in the derivative TG curve (dTG) or mechanistic methods such as evolved gas analysis (EGA) [14]. In fire modelling, the kinetics are implemented for example in the species mass conservation equation, to be able to capture the mass loss due to thermal decomposition [1,31]. Many pyrolysis models employ an n-th order scheme [1], though real behaviour may deviate [32–34].

Experimental Boundary Conditions

Reliable kinetic parameters require experiments that satisfy the 0D assumption, i.e. decomposition governed solely by intrinsic kinetics. The ICTAC guidelines provide detailed recommendations [14], while equivalent standards for fire science are still lacking.

Accurate mass and temperature measurements are essential. Blank-curve correction compensates buoyancy effects, and temperature calibration is typically performed with Curie points or pure metals [16]. However, differences between calibration and sample properties and endo-/exothermic effects during decomposition can still introduce errors.

Heat transfer within the sample is another critical factor. Below 800 °C, conduction dominates, making the thermal diffusivity of sample, crucible and purge gas important [35]. Sample size, geometry and heating programme affect the effective heating rate. Such influences cannot be eliminated and must be considered when interpreting results.

Atmosphere composition and purge flow can significantly alter decomposition behaviour. Partial pressures of evolved gases may slow or accelerate reactions,

corresponding to the pressure term $h(p)$ in Eq. (2). Purge flow rates should therefore be set high enough to keep concentration effects negligible [5,14].

Both non-isothermal and isothermal experiments are used in kinetic studies [19]. Non-isothermal runs may suffer from differences between nominal and effective heating rates due to thermal gradients. In isothermal experiments, achieving and maintaining the target temperature is difficult, and decomposition may already occur during heating. These effects complicate interpretation, especially for multi-step processes.

The ICTAC recommendations propose a downscaling approach with respect to sample mass. Starting from an initial mass that should be as small as possible, the sample mass is further reduced until congruent curves are obtained. Only in this way can it be ensured that no transport phenomena systematically distort the results [14].

Some systematic deviations in thermoanalytical results are to be expected. For instance, a shift of the TG signal can be observed when the heating rate is increased. In the case of a decomposition reaction that proceeds through independent steps, however, a change in the slope of the TG signal would indicate the occurrence of undesired effects, where the 0D assumption is no longer valid [14].

MATERIAL AND METHODS

Material and Sample Preparation

Black cast PMMA was used in this study as a sample material (trade name PLEXIGLAS GS black 9H01 by Röhm), because it has a non-complex decomposition behaviour while still decomposing in a multi-step process. The divergent standards of thermoanalytical and calorimetric methods permit a range of sample configurations [7,15,16]. In principle, a representative form should be selected, which in the case of a PMMA sheet could be a piece. However, some authors recommend the use of powder [17]. Therefore, two configurations (powder and piece) were explicitly selected and analysed as relevant sample configurations. The material was sourced from a 6 mm thick PMMA sheet. Pieces were produced using diagonal pliers, while powder was obtained by milling the material into shavings, followed by manual grinding with a mortar. Using laboratory sieves, the ground powder was separated into a particle size fraction of 75-250 µm. All samples were handled and processed with utmost care to avoid temperature increases that could alter material properties and to prevent contamination.

For each experiment, crucibles were filled with a sample mass close to the specified nominal value (m_0) with deviations ≤ ± 6 % of the nominal sample mass (measurement uncertainty ± 0.01 mg). While the required mass was straightforward to weigh for the powder samples, one to two small pieces were

typically used in the piece experiments to achieve the nominal mass. All samples were conditioned in accordance with ISO 291 (standard climate: 23 ± 2 °C, 50 ± 10 % RH) and subsequently stored in a desiccator for a minimum of one week [36].

Experimental Programme and Analysis

The thermal decomposition of PMMA was investigated using an STA device (TGA/DSC 3+, Mettler Toledo). The instrument is a horizontally supported TG apparatus with positions for both a reference and a sample crucible (Fig. 1). A thermocouple (TC) positioned beneath the reference crucible measures the furnace temperature (RTC), while the sample temperature is measured by TC beneath the sample crucible (STC). In addition to recording the mass signal as a function of time and temperature, the arrangement of thermocouples within the sample holder allows the derivation of a heat flow signal (DTA). For the derivation of the kinetic model, however, only the TG data were used.

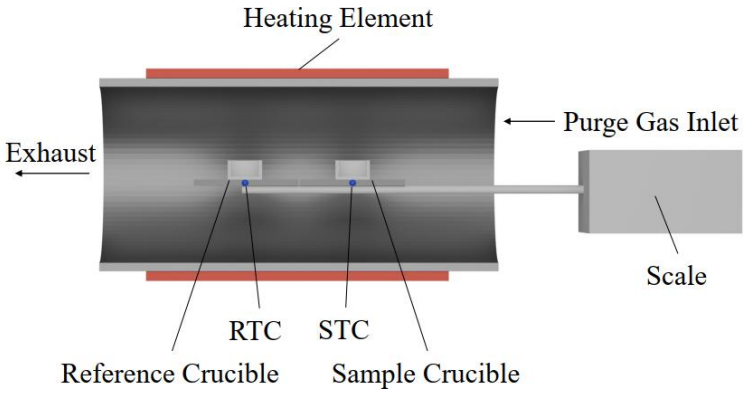

Figure 1: Schematic diagram of the horizontally supported STA apparatus with two thermocouples to measure sample and reference temperature.

Mass and temperature calibrations were performed before measurements in accordance with relevant standards [15,16]. The balance was calibrated using the instrument's internal function, and indium and aluminium were used for temperature and heat flow calibration. Blank curves were recorded and subtracted to compensate for buoyancy effects. The STA was mounted on a vibration isolation platform to optimise signal fidelity and minimise environmental interference. Each experimental configuration was repeated three times to ensure data quality and statistical reliability.

All experiments were conducted with a nitrogen purge gas flow rate of 40 mL/min. A settling phase prior to the start of the experiment was used to ensure a fully inert atmosphere [16].

Initially, samples in piece and powder form with masses between 1 and 12 mg were examined, until an appropriate nominal mass was identified through the study of mass effects. The effect of heating rate was studied in non-isothermal experiments at 5-60 K/min from 90 °C to 700 °C, followed by a 15 min hold to

ensure complete decomposition. 70 µL alumina crucibles with a height-to-diameter ratio of 0.75 were used for all STA experiments. For selected conditions, the purge gas flow rate was also varied to investigate these effects.

Isothermal experiments were performed to obtain information on the reaction model [19]. Following the ICTAC recommendations [14], the isothermal temperature should be chosen such that the heating phase is minimised while excessively long holding times are avoided. A good starting point is a conversion level between 5 and 10 %. Starting from this temperature, higher values may be applied to further shorten the holding phase.

For the isothermal experiments, a 15-minute settling time at 120 °C was applied, followed by heating to the target isothermal temperature at the maximum heating rate. The temperature was then held constant for 480 minutes. An initial isothermal temperature of 300 °C was selected, as the conversion at this point was within the recommended range (9.28% for the powder sample and 7.70% for the piece sample). However, since the conversion remained below 0.7 during the holding period, additional isothermal experiments were conducted at 320 °C, yielding conversion values of 14.01% for the powder sample and 11.25% for the piece sample.

In selected STA experiments, evolved gas analysis (EGA) with a Fourier-transform infrared (FTIR) spectrometer was conducted to investigate the decomposition mechanism of PMMA. FTIR spectra in the range of 400 to 4000 cm^{-1} (resolution: 4 cm^{-1}, optical path length: 100 mm, heated system at 240 °C) were recorded, from which Gram-Schmidt curves and chemigrams for specific wavelengths could be derived. In addition, a NIST database search was carried out to identify the gaseous components.

The analysis considered the time- and temperature-resolved mass ($m(\cdot)$) as well as the differential thermogravimetric signal ($\mathrm{d}m/\mathrm{d}t$). Settling periods were excluded. For non-isothermal data, values below a sample temperature of 130 °C were removed, as the transition from the settling to the heating phase introduced artefacts that hindered automated evaluation. Normalised values are marked with an asterisk (*). In addition to descriptive statistics, including the mean (avg, bar notation) and standard deviation (std, σ), selected aspects were evaluated using inferential methods, primarily ANOVA and Tukey's HSD test, implemented in the Python libraries SciPy (version 1.10.1) [37] and statsmodels (version 0.14.4) [38]. Methodological details are given in [39-41]. A p-value of 0.05 was taken as the threshold for statistical significance.

Kinetic Parameter Estimation and Performance Analysis

The multi-step nature of PMMA decomposition was confirmed through an isoconversional analysis using the KAS method with the Starink approximation, as implemented in FireSciPy [42]. Based on the experimental sensitivities, the data from the non-isothermal experiments with heating rates of 5, 10, 20, and 30 K/min were used for this purpose. For parameter estimation, an optimisation

workflow was developed in which a Differential Evolution algorithm (SciPy [37]) was coupled with the Fire Dynamics Simulator (FDS, revision 6.10.1-0-g12efa16-release).

With the workflow, kinetic parameters (E_a, A, n) and mass fractions (Y) associated with the individual decomposition (i) steps were determined. In the simulation, the TGA mode implemented in FDS was used to reproduce such an experiment, and the course of dm/dt was compared with the experimental data (β = 30 K/min). The optimisation objective was to minimise the sum of squared errors (SSE). Given the different decomposition steps of powder and piece samples, two separate parameter sets were defined and examined in a performance analysis.

Three cases were considered in the performance analysis (Fig. 2):

a) Gasification experiments of 10 × 10 × 2 cm³ specimens, horizontally oriented and exposed on one side to heat fluxes of 20, 25, 40, 50, and 75 kW/m². Simulations used the solid-phase-only mode in FDS.

b) Cone calorimeter experiments under identical boundary conditions as in a), but including gas-phase combustion.

c) A 35 × 10 × 2 cm³ specimen was irradiated with 50 kW/m² on a 5 × 10 cm² area located at one end. The remainder of the surface was exposed to a uniform pre-heating flux of 10 kW/m², enabling horizontal fire spread across the specimen.

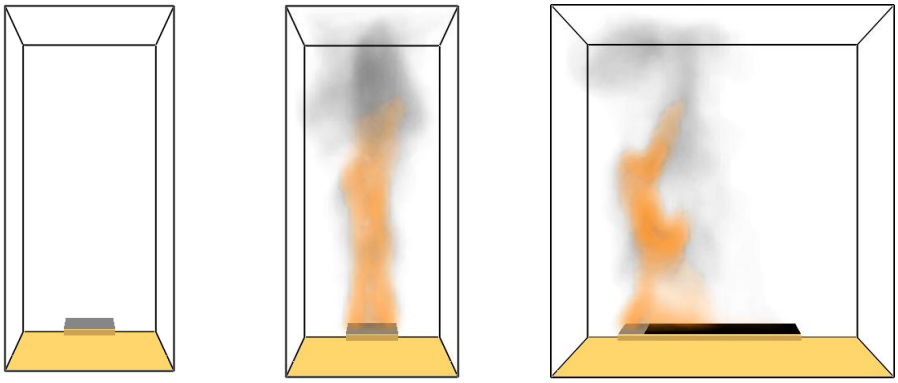

Figure 2: Visualisation of the simulation setups (a) Gasification experiment (b) Cone calorimeter experiment (c) Fire spread case.

Unless stated otherwise, default values and models in FDS were used [43,44]. The simulations employed a cubic fluid mesh with a cell edge length of 10 mm and were performed in large eddy simulation (LES) mode. The number of radiation angles was increased to 1000 and solid-phase updates were carried out at every time step. In this study, only kinetic parameters were varied, while all other thermophysical properties of PMMA and the fuel properties, assumed to be methyl methacrylate (MMA), were adopted from the NIST/NRC parallel panel

validation case (GitHub commit a0d5df3) [45]. The backside of all specimen was assumed to be insulated.

RESULTS

General Decomposition Behaviour

The two sample configurations exhibit distinct decomposition behaviours (Fig. 3). For powder, a pronounced mass-loss peak occurs between 170 and 220 °C, while the piece shows only a gradual increase in mass loss. In both cases, a slow, steady mass loss continues up to 300 °C, followed by a shoulder peak preceding the main decomposition peak. Although this multi-step mechanism has been reported previously [46-48], it appears less pronounced for the pieces.

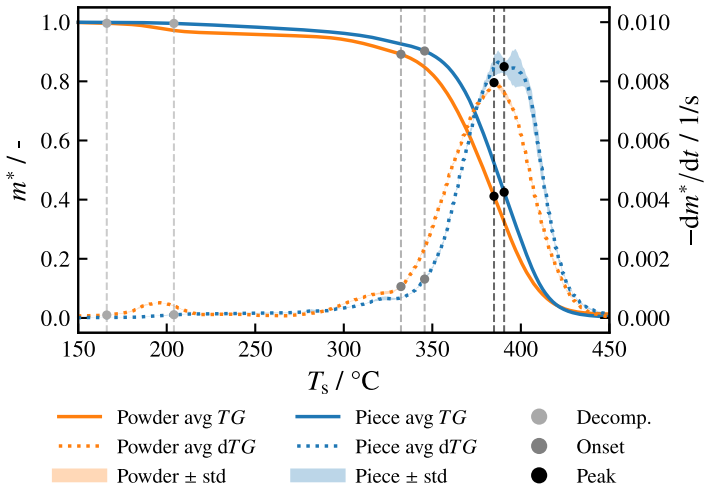

Figure 3: Comparison of the decomposition behaviour of powder and piece (m_0 = 3 mg, β = 30 K/min) with indication of characteristic values.

These differences can be quantified by characteristic values. For nominal sample masses of 3 mg and at a heating rate of 30 K/min, the decomposition temperature (initial mass loss, threshold: 1.2 % of maximum dTG) differs by 38.0 °C. The onset temperature (beginning of main mass loss) differs by 13.4 °C, and the peak temperature (global mass-loss maximum) by 5.8 °C.

In the isoconversional analysis, the presence of a multi-step process was confirmed (Fig. 4). The course of apparent conversion dependent activation ($\mathrm{E}_{\propto,\mathrm{a}}$) energy is clearly non-constant. The relative range within $0.05 \leq \alpha \leq 0.95$ was 68.54 % for powder ($\bar{E}_{\propto,\mathrm{a,powder}}$ = 226.15 kJ/mol) and 58.21 % for piece ($\bar{E}_{\propto,\mathrm{a,piece}}$ = 204.83 kJ/mol), exceeding the 10-20 % criterion for multi-step behaviour [25]. This is consistent with the multiple peaks observed in the dTG data.

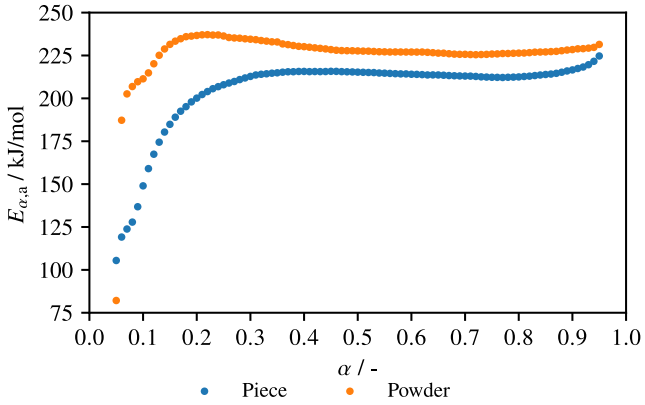

Figure 4: Apparent conversion-dependent activation energy ($E_{\propto,a}$) curves for both sample configurations for m_0 = 3 mg.

Step-specific mass losses could not be directly determined from STA data, because of overlapping decomposition processes and the absence of isolated peak patterns. PMMA is generally assumed to decompose without leaving a residue [49]. In some cases, a slight black residue was visible in the crucibles. Subsequent measurements of the residual mass showed values below the measurement uncertainty of the laboratory balance (≤ 0.01 mg), suggesting that any remaining residue is negligible.

Evolved gas analysis under inert conditions qualitatively identified methyl methacrylate (MMA), carbon dioxide (CO_2), and water vapor. According to Zeng et al. [50], MMA is the main decomposition product, which further degrades into smaller molecules, including CO_2. The present results are therefore consistent with the existing literature. The chemigrams for MMA (1060–1260 cm^{-1}) and CO_2 (2200–2500 cm^{-1}) show that their release is directly correlated with the mass loss. A stepwise evolution of specific components, which would manifest as distinct peaks in the chemigrams, could not be observed.

Influence of Experimental Boundary Conditions

To investigate the influence of sample mass, non-isothermal experiments with different nominal masses were conducted. Starting from 12 mg, the mass was gradually reduced to 6, 3, 2, and 1 mg until congruent curves were observed. Since excessive mass is particularly critical at higher heating rates, these experiments were performed at the two highest heating rates used (30 and 60 K/min) (Fig. 5). The results, presented as dTG curves of the main decomposition peak, show that congruence is not achieved at 60 K/min, but only at 30 K/min and for sample masses of 3 mg or less. The latter boundary conditions ensure that the 0D assumption holds. The congruence of peak profiles was also confirmed by ANOVA and Tukey's HSD test. Furthermore, the statistical analysis revealed that in the powder configuration larger deviations between the different mass groups occur. In addition to a shift in peak temperature, increased sample masses also led to peak broadening.

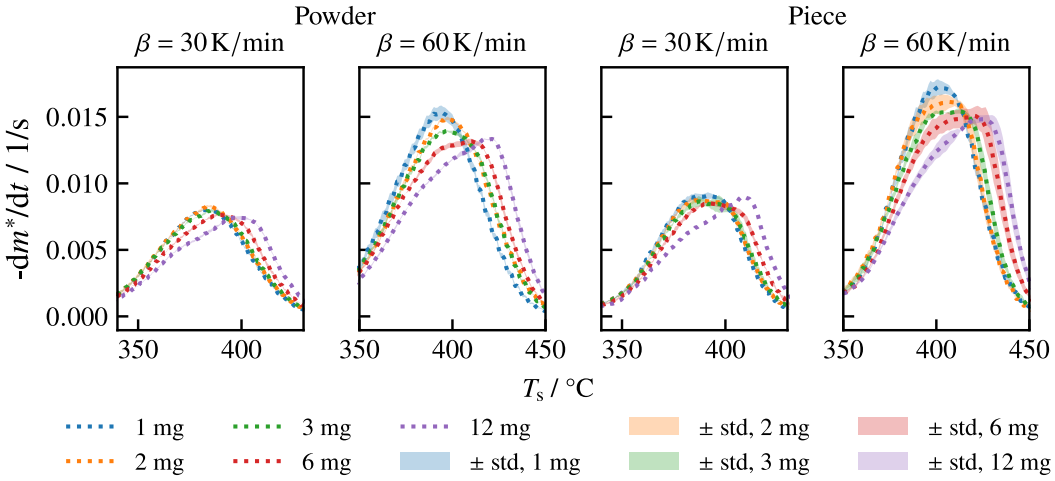

Figure 5: Comparison of different nominal masses at heating rates of 30 and 60 K/min for both sample configurations. Focus on main decomposition peak.

An increase in heating rate at constant sample mass is known to shift TG data [14], but it should not affect the overall curve shape, such as the slope of $m(T)$. For sample masses of 1 and 2 mg, no relevant deviations were observed at the different heating rates, whereas for 3 mg such effects were apparent at 60 K/min. The occurance of slope changes in $m(T)$ at 60 K/min for both sample configurations demonstrated that these high heating rate introduces – at least in the case of the used sample mass – systematic deviations.

From the investigations of sample mass and heating rate, it was concluded for all subsequent experimental studies and analyses that the maximum valid sample mass is 3 mg and the heating rate should be ≤ 30 K/min.

When evaluating the peak temperatures at heating rates of 5-30 K/min for m_0 = 3 mg, it becomes apparent that the peak temperature shift is larger for the piece configuration than for the powder (27.5 °C vs. 24.5 °C). Other potential heating rate effects were not identified. A change in the course of reaction with varying heating rate could, for instance, point to a consecutive reaction [30]. In the present case, however, no such effect was observed.

The products formed during decomposition can influence the overall decomposition mechanism [19]. In Eq. 2, this is reflected, for example, by the effect of a partial pressure of an evolved gas. To investigate such a potential influence, the purge gas flow rate was varied (Fig. 6). A relevant effect was observed only for the powder configuration, and only in the region of the first mass-loss peak. ANOVA of the dTG values at 190 °C confirmed this finding. A shift of the small peak towards higher temperatures was observed as the flow rate decreased. According [14], this indicates a reversible reaction in which efficient removal of the evolved gaseous products accelerates the reaction.

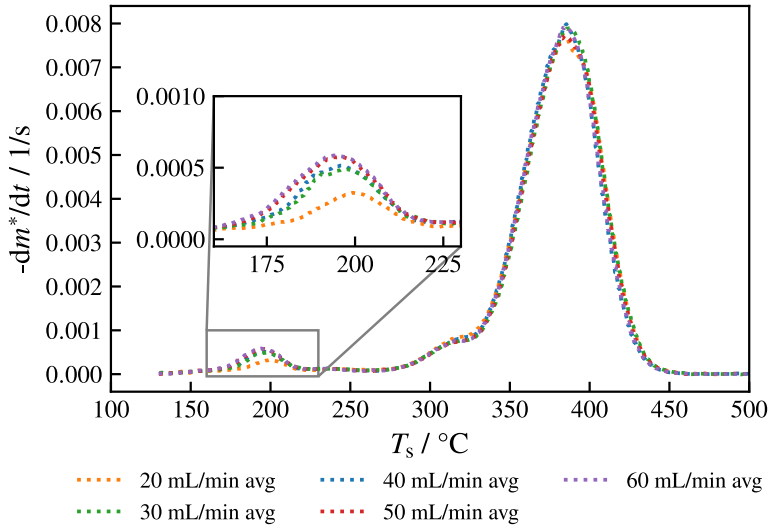

Figure 6: Influence of the purge gas flow rate on the dTG course for powder (m_0 = 3 mg, β = 30 K/min).

Kinetic Parameter Determination

The experimental data provided relevant insights for kinetic modelling. Separate parameter sets were required for the two sample configurations. PMMA decomposition was represented as complete, without residual mass. The individual steps of the multi-step decomposition were found to be independent and were therefore modelled as parallel reactions. For both piece and powder, four decomposition steps were assumed, based on the characteristics observed in the dTG data (Fig. 3).

For the description of a thermal decomposition, various reaction models exist. However, FDS provides only a single implemented option. This is an nth-order model, which is useful for describing decelerating reactions. To assess its applicability, isothermal TGA experiments were conducted. As shown in Fig. 7, the decomposition exhibits a decelerating behaviour. The isothermal data after the settling phase (after t = 900 s) are shown. The deviation at the beginning is due to the non-isothermal phase during heating to the isothermal temperature.

The optimisation results are presented in Fig. 8 and Tabs. 1 and 2. Using four decomposition steps, all kinetic parameters required for modelling the decomposition of both sample configurations were successfully determined. The deviations between the simulations and the experimental target data are minimal, with a root mean squared error (RMSE) of $2.08 \cdot 10^{-5}$ 1/s for the powder configuration and $3.26 \cdot 10^{-5}$ 1/s for the piece configuration. It should be noted that the kinetic parameters are not unique, for example due to the kinetic compensation effect [51].

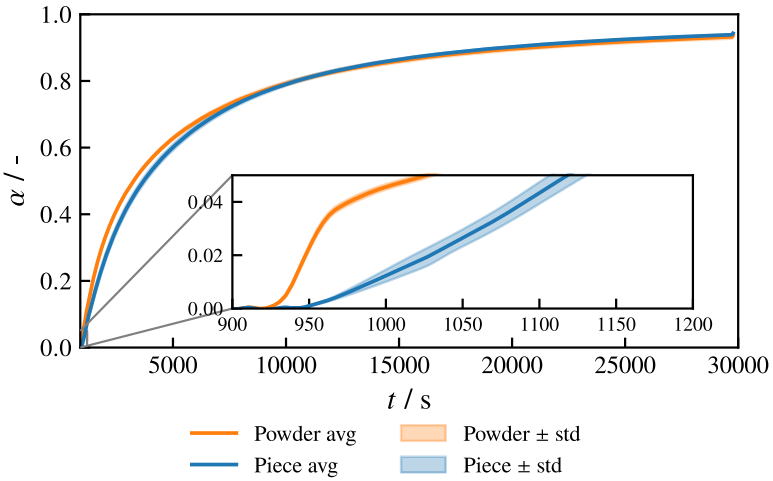

Figure 7: Isothermal experiment with temperature of 320 °C for both sample configurations (m_0 = 3 mg).

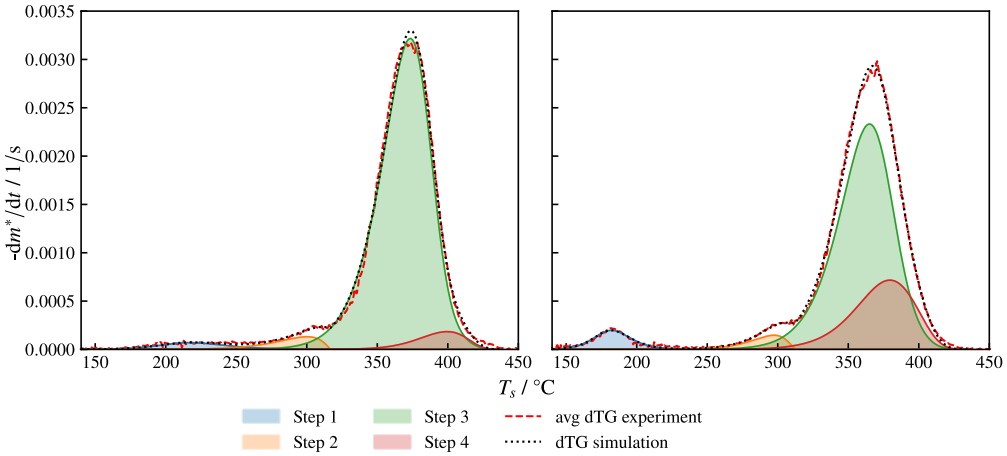

Figure 8: Optimisation results: Individual decomposition steps and comparison of simulated and experimental mass loss rate of piece (left) and powder (right) (m_0 = 3 mg, β = 30 K/min).

Performance Analysis

The results of the gasification simulations (Fig. 9) clearly show that the kinetic parameters of the powder lead to an accelerated decomposition compared with those of the piece configuration. This effect is particularly pronounced at lower incident heat fluxes. For example, at a heat flux of 20 kW/m², complete decomposition at the specimen centre occurs 225.78 s earlier with the parameters derived from the powder dataset than with those from the piece configuration. At 75 kW/m², the difference is reduced to only 6.05 s.

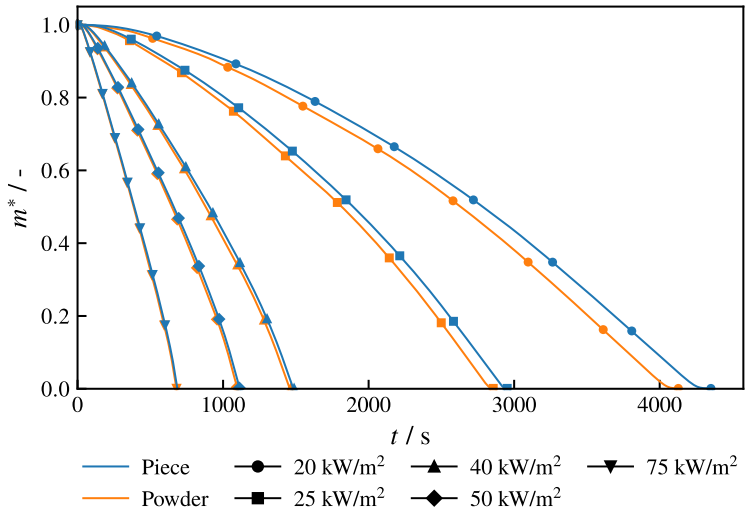

Figure 9: Normalised mass vs. time for different incident heat fluxes and both sample configurations (gasification case). Measurement in the centre of the plate.

In the cone calorimeter setups (Fig. 10), the final difference is smaller due to the additional heat flux from flaming combustion. At 20 kW/m², however, the specimen ignites earlier with the powder parameters than with those of the piece configuration.

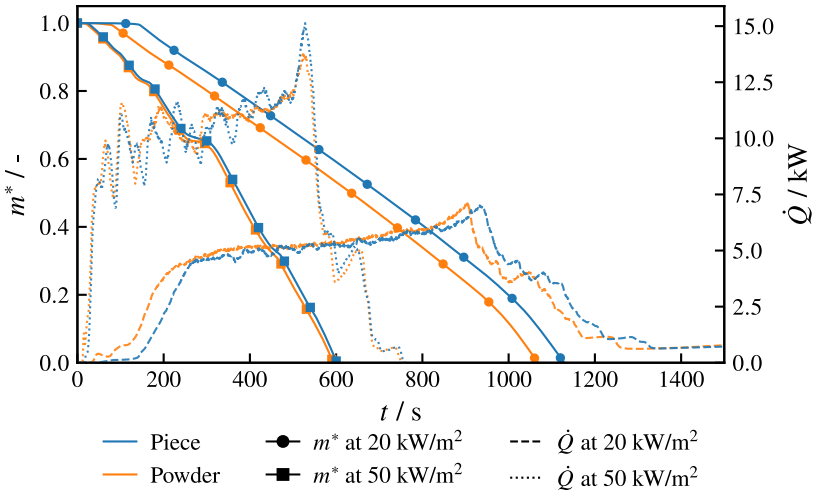

Figure 10: Normalised mass and heat release rate vs. time for different incident heat fluxes and both sample configurations (cone calorimeter case). Mass measurement in the centre of the plate.

Figure 11 presents the results of the spread simulation case, showing the decomposition front propagating along the central axis of the plate. This represents not the flame front, but the spatial progression of material decomposition. The kinetic model derived from the powder results in a markedly

faster spread of decomposition (average velocity: powder 0.3586 cm/s; piece 0.2119 cm/s).

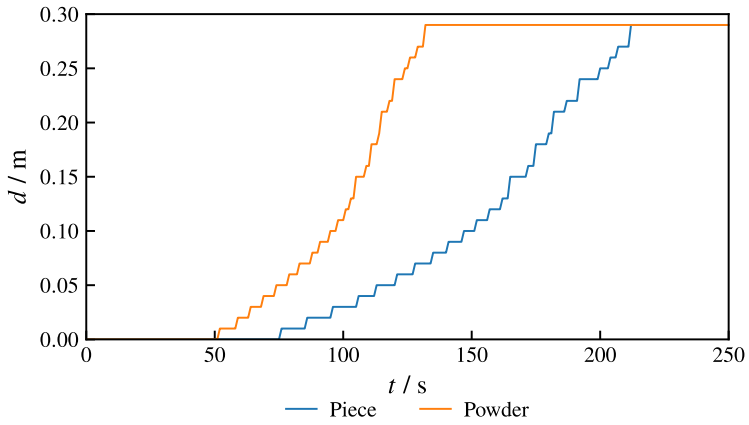

Figure 11: Time-resolved position of the decomposition front.

DISCUSSION & CONCLUSION

Influences of Experimental Boundary Conditions

The comprehensive investigation of experimental boundary conditions demonstrated that some of these factors substantially influence the course of decomposition reactions, most notably the sample configuration. According to common standards, e.g. for DSC [15] or TGA [16], the sample form is not strictly defined but rather required to be representative. However, the present results clearly show that two configurations, such as powder and piece, can lead to fundamentally different decomposition behaviours.

The effects of heating rate and sample mass were further examined, enabling the identification of the critical combination beyond which the fundamental assumption of microscale experiments (0D behaviour) no longer holds. In the present study, this limitation was addressed by restricting the analysis to heating rates of up to 30 K/min and sample masses not exceeding 3 mg.

Beyond their systematic impact, the variation of boundary conditions also provided important mechanistic insights into the decomposition process. In particular, it allowed testing whether consecutive decomposition steps may be present, which would have been reflected in a pronounced heating rate dependence. Together with the evolved gas analysis (EGA), which supplied further mechanistic information, these investigations were crucial for establishing a sound basis for the subsequent kinetic modelling.

Some authors have already addressed the issue of heat conduction in microscale experiments [52], and the microscale combustion standard also provides recommend-dations [7]. However, experimental investigations, such as those

conducted in this study, remain indispensable. For example, the analysis in [52] was based on a purely theoretical approach for two polymers, assuming a slab geometry and one-dimensional heat conduction. The extent to which such results can be transferred to other sample configurations and materials remains uncertain.

As there are currently no established experimental standards for the determination of pyrolysis model parameters within the fire science community, it is recommended to consistently refer to the ICTAC guidelines [14]. The ICTAC recommendations provide a widely accepted scientific basis for the design and interpretation of such experiments and were explicitly taken into account in the present study.

Physical Constraint

It remains unclear why the decomposition behaviour of powder and piece, particularly at the onset, differs so markedly, despite both being composed of the same material. Similar differences in the decomposition of PMMA were reported by DiDomizio and McKinnon, who observed variations depending on the cryo-milling duration that produced different particle sizes, yet could not identify the underlying reason [18].

One possible explanation for the delayed decomposition in the case of the piece configuration could be heating effects. However, the decomposition pattern remained unchanged across different masses and heating rates. In the present case, it was demonstrated that transport-related limitations only arise when masses exceed 3 mg and heating rates exceed 30 K/min. Heating effects therefore do not explain these differences.

As an example, from a different material, Oswald and Wiedemann investigated cobalt hydroxy-sulphate hydrates with particle sizes ranging from 0.3 to 250 µm and found that the onset time strongly depended on particle size [53]. In their case, nucleation of the product phase controlled the process for small particles, whereas diffusion of water molecules became rate-limiting for larger particles. In this example, the particle sizes determined the processes that took place.

In the present study, the results point instead towards a restriction of gas release as the governing factor, at least for the beginning of the decomposition. The influence of purge gas flow rate supports this hypothesis: the initial decomposition peak of the powder configuration was shifted to higher temperatures at lower flow rates, whereas the piece remained unaffected. This indicates that in the powder configuration, the larger surface-to-volume ratio facilitates faster gas release. At low flow rates, however, partial pressure effects can build up and alter the reaction. For the piece, such effects appear negligible. For the pieces, this would mean that gas release is impeded. The very small but steady increase in the mass loss rate in the case of pieces underscores this assumption. At higher temperatures, the difference between both sample configurations vanishes, as the material melt and gas transport becomes dominated by convection. Further

investigations are required to confirm the role of gas-release restriction in governing the observed differences. In addition, its relevance for kinetic modelling remains to be clarified.

Kinetic Modelling and Fire Simulations

For both sample configurations, kinetic models were successfully established using the optimisation workflow, each capturing the decomposition in four independent steps.

The key difference in the decomposition behaviour of powder and piece is the first mass-loss peak of the powder in the range of 170-220 °C. Although only about 5 % of the mass is decomposed in this step, the performance analysis demonstrated that it has a significant influence. In particular, the effect is most pronounced at low heat fluxes, where the slower heating rate of the material causes the kinetic parameters derived from the powder configuration to lead to faster decomposition compared with those of the piece configuration. In the horizontal spread simulation, this resulted in a markedly reduced decomposition front velocity when using the piece parameters. Overall, the performance analysis clearly highlighted the critical importance of the experimental data on which the kinetic parameters are based.

OUTLOOK

This study has shown that micro-scale experiments designed to derive kinetic parameters must be conducted with great care. Boundary conditions need to be well controlled and clearly defined in order to generate reliable data. It was demonstrated that the ICTAC recommendations provide a relevant contribution to ensuring high data quality. Although the reasons why piece and powder samples yield such different results could not be fully clarified, the successful determination of kinetic parameters allowed the performance analysis to demonstrate the effects of the two sample configurations. Further investigations are required in this regard. For modelling practice, validation studies are needed to determine which sample configurations provide more reliable data for the derivation of kinetic parameters.

ACKNOWLEDGEMENTS

This contribution contains aspects that have been examined in greater detail in [54], to which the interested reader is referred. The work was partly supported by the German Federal Ministry of Research, Technology and Space (BMFTR) through the project BESKID (grant numbers 13N16390, 13N16392).

CRediT authorship contribution statements: Felix Armbrust: Conceptualisation, methodology, investigation, analysis, writing – original draft, review & editing; Tristan Hennen: Conceptualisation, writing – review & editing; Jochen Zehfuss:

Supervision, writing – review & editing; Olaf Riese and Lukas Arnold: Writing – review & editing

LITERATURE

[1] Stoliarov S.I., Ding Y. Pyrolysis model parameterization and fire growth prediction: The state of the art. Fire Saf. J., 140(2023).

[2] Nyazika T., Jimenez M., Samyn F., Bourbigot S. Pyrolysis modeling, sensitivity analysis, and optimization techniques for combustible materials: A review. J. Fire Sci., 37(2019).

[3] Matala A. Methods and applications of pyrolysis modelling for polymeric materials. Dissertation, Aalto University, 2013.

[4] West P.W. Inorganic thermogravimetric analysis. J. Chem. Educ., 1954.

[5] Coats A.W., Redfern J.P. Thermogravimetric analysis. Analyst, 1963.

[6] Lyon R.E., Walters R.N. Pyrolysis combustion flow calorimetry. J. Anal. Appl. Pyrolysis, 71(2004).

[7] ASTM International. Standard test method for determining flammability characteristics of plastics and other solid materials using microscale combustion calorimetry (ASTM D7309-21b). ASTM Int., 2021.

[8] Girardin B., Fontaine G., Duquesne S., Försth M., Bourbigot S. Characterization of thermo-physical properties of EVA/ATH: Application to gasification experiments and pyrolysis modeling. Mater., 8(2015).

[9] Ding Y., McKinnon M.B., Stoliarov S.I., Fontaine G., Bourbigot S. Determination of kinetics and thermodynamics of thermal decomposition for polymers containing reactive flame retardants: Application to poly(lactic acid) blended with melamine and ammonium polyphosphate. Polym. Degrad. Stab., 129(2016).

[10] DiDomizio M.J., McKinnon M.B., Bellamy M. Measurement of thermal conductivity of thermally reactive materials for use in pyrolysis models. Fire Mater. 48(2024).

[11] ASTM International. Obtaining data for fire growth models (STP1642-EB). ASTM Int., 2023.

[12] Hehnen T., Arnold L. PMMA pyrolysis simulation – from micro- to real-scale. Fire Saf. J. 141(2023).

[13] IAFSS. Measurement computation of fire phenomena (MaCFP Working Group). https://iafss.org/macfp/ [online]. 2025.

[14] Vyazovkin, S., Chrissafis, K., Di Lorenzo, M.L., Koga, N., Pijolat, M., Roduit, B., Sbirrazzuoli, N., Suñol, J.J. ICTAC Kinetics Committee recoomendations for collecting experimental thermal analysis data for kinetic computations. Thermochim. Acta, 590(2014).

[15] ISO. Plastics – Differential scanning calorimetry (ISO 11357-1:2023). ISO, 2023.

[16] ISO. Plastics – Thermogravimetry (ISO 11358-1:2022). ISO, 2022.

[17] Brown M. Introduction to thermal analysis. Kluwer Acad. Publ., 2004.

[18] DiDomizio M.J., McKinnon M.B. Impact of specimen preparation method on thermal analysis testing and derived parameters. ASTM Int., 2023.

[19] Vyazovkin S., Burnham A.K., Criado J.M., Pérez-Maqueda L.A., Popescu C., Sbirrazzuoli N. ICTAC Kinetics Committee recommendations for performing kinetic computations on thermal analysis data. Thermochim. Acta, 520(2011).

[20] Vyazovkin S. Computational aspects of kinetic analysis: Part C. The ICTAC kinetics project – the light at the end of the tunnel?. Thermochim. Acta, 355(2000).

[21] Vyazovkin S., Wight C.A. Model-free and model-fitting approaches to kinetic analysis of isothermal and nonisothermal data. Thermochim. Acta, 340(1999).

[22] Vyazovkin S. Model-free kinetics: Staying free of multiplying entities without necessity. J. Therm. Anal. Calorim., 83(2006).

[23] Vyazovkin S. Isoconversional kinetics. In: Recent advances, techniques and applications. Elsevier, Amsterdam, 2008.

[24] Vyazovkin S. Isoconversional kinetics of thermally stimulated processes. Springer Cham, 2015.

[25] Vyazovkin S. Kissinger method in kinetics of materials: Things to beware and be aware of. Molecules, 25(2020).

[26] Pielichowski K., Njuguna J., Majka T.M. Thermal degradation of polymeric materials. Elsevier, Amsterdam, 2022.

[27] Koga N., Vyazovkin S., Burnham A.K., Favergeon L., Muravyev N.V., Pérez-Maqueda L.A., Saggese C., Sánchez-Jiménez P.E. ICTAC Kinetics Committee recommendations for analysis of thermal decomposition kinetics. Thermochim. Acta, 719(2023).

[28] Starink M.J. The determination of activation energy from linear heating rate experiments: a comparison of the accuracy of isoconversion methods. Thermochim. Acta, 404(2003).

[29] Opfermann J. Kinetic analysis using multivariate non-linear regression. I. Basic concepts. J. Therm. Anal. Calorim. 60(2000).

[30] Moukhina E. Determination of kinetic mechanisms for reactions measured with thermoanalytical instruments. J. Therm. Anal. Calorim., 109(2012).

[31] Moghtaderi B. Pyrolysis of char forming solid fuels: A critical review of the mathematical modelling techniques. Proc. 5th Asia-Oceania Symp. Fire Sci. Technol., IAFSS, 2001.

[32] Sánchez-Jiménez P.E., Pérez-Maqueda L.A., Perejón A., Criado J.M. Combined kinetic analysis of thermal degradation of polymeric materials under any thermal pathway. Polym. Degrad. Stab., 94(2009).

[33] Snegirev A.Y., Talalov V.A., Stepanov V.V., Korobeinichev O.P., Gerasimov I.E., Shmakov A.G. Autocatalysis in thermal decomposition of polymers. Polym. Degrad. Stab. 137(2017).

[34] Snegirev A.Y., Talalov V.A., Stepanov V.V., Harris J.N. Formal kinetics of polystyrene pyrolysis in non-oxidizing atmosphere. Thermochim. Acta, 548(2012).

[35] Brown M. (ed.). Handbook of thermal analysis and calorimetry. Vol. 1. Elsevier, Amsterdam, 1998.

[36] ISO. Plastics – Standard atmospheres for conditioning and testing (ISO 291:2008). ISO, 2008.

[37] Virtanen P., et al. SciPy 1.0: Fundamental algorithms for scientific computing in Python. Nat. Methods, 17(2020).

[38] Seabold, S., Perktold, J. Statsmodels: Econometric and statistical modeling with python. Proc. of the 9th Python in Science Conf. 2010.

[39] Herzog M.H., Francis G., Clarke A. Understanding statistics and experimental design. Springer Cham, 2019.

[40] Lane, D.M. Online Statistics Education: An Interactive Multimedia Course of Study. Rice University, University of Houston Clear Lake, Tufts Universtiy. https://onlinestatbook.com/2/index.html [online]. 2025.

[41] Guthrie W.F. NIST/SEMATECH e-Handbook of statistical methods. NIST, Gaithersburg, 2020.

[42] Hehnen T. FireSciPy: Fundamental algorithms from the field of fire science, for computations with Python. https://github.com/FireDynamics/FireSciPy [online]. 2025.

[43] McGrattan, K., Hostikka, S., Floyd, J., McDermott, R., Vanella, M., Mueller, E., Paul, C. Fire Dynamics Simulator User's Guide. Revision: FDS-6.10.1-0-g12efa16. 2025.

[44] McGrattan, K., Hostikka, S., Floyd, J., McDermott, R., Vanella, M., Mueller, E., Paul, C. Fire Dynamics Simulator Technical Reference Guide Volume 1: Mathematical Model. Revision: FDS-6.10.1-0-g12efa16. 2025.

[45] McGrattan, K., Hostikka, S., Floyd, J., McDermott, R., Vanella, M., Mueller, E., Paul, C. Fire Dynamics Simulator Technical Reference Guide Volume 3: Validation. Revision: FDS-6.10.1-0-g12efa16. 2025.

[46] Hirata T., Kashiwagi T., Brown J.E. Thermal and oxidative degradation of poly(methyl methacrylate) molecular weight. Macromolecules, 18(1985).

[47] Holland B.J., Hay J.N. The effect of polymerisation conditions on the kinetics and mechanisms of thermal degradation of PMMA. Polym. Degrad. Stab., 77(2002).

[48] Ferriol M., Gentilhomme A., Cochez M., Oget N., Mieloszynski J.L. Thermal degradation of poly(methyl methacrylate) (PMMA): modelling of DTG and TG curves. Polym. Degrad. Stab., 79(2003).

[49] Salgansky E.A., Salganskaya M.V., Glushkov D.O., Pleshko A.O. The experimental study of the kinetics and modes of polymethyl methacrylate thermal degradation in argon flows. Thermochim. Acta, 736(2024).

[50] Zeng W.R., Li S.F., Chow W.K. Review on chemical reactions of burning poly(methyl methacrylate) PMMA. J. Fire Sci., 20(2002).

[51] Lesnikovich, A.I., Levchik, S.V. A method of finding invariant values of kinetic parameters. J. Therm. Anal., 27(1983).

[52] Lyon R.E., Safronava, N., Senese, J., Stoliarov, S.I. Thermokinetic model of sample response in nonisothermal analysis. Thmerochim. Acta, 545(2012).

[53] Oswald H.R., Wiedemann H.G. Factors influencing thermoanalyical curves. J. Therm. Anal. 12(1977).

[54] Armbrust, F., Hehnen, T., Zehfuß, J., Riese, O., Arnold, L. Discrepancies and experimental influences in micro-scale measurements for kinetic modelling. LeoPARD TU Braunschweig Publications and Research Data, 2025.

APPENDIX: KINETIC PARAMETERS

Table 1: Kinetic parameters for the piece configuration.

Step (i)	$Y_{i,s}$ (-)	A_i (1/s)	$E_{a,i}$ (kJ/mol)	n_i (-)
1	$2.64 \cdot 10^{-2}$	$1.02 \cdot 10^{10}$	130.92	2.29
2	$3.30 \cdot 10^{-2}$	$1.07 \cdot 10^{10}$	124.73	0.52
3	$8.93 \cdot 10^{-1}$	$1.00 \cdot 10^{10}$	203.67	2.45
4	$4.76 \cdot 10^{-2}$	$4.79 \cdot 10^{18}$	259.75	0.81

Table 2: Kinetic parameters for the powder configuration.

Step (i)	$Y_{i,s}$ (-)	A_i (1/s)	$E_{a,i}$ (kJ/mol)	n_i (-)
1	$4.09 \cdot 10^{-2}$	$9.63 \cdot 10^{18}$	196.97	2.11
2	$2.90 \cdot 10^{-2}$	$3.48 \cdot 10^{14}$	174.10	0.64
3	$6.97 \cdot 10^{-1}$	$1.00 \cdot 10^{10}$	193.46	2.28
4	$2.33 \cdot 10^{-1}$	$6.56 \cdot 10^{13}$	186.61	0.63